Korean J. Chem. Eng., 33(3), 893-901 (2016)
DOI: 10.1007/s11814-015-0196-6

pISSN: 0256-1115
eISSN: 1975-7220

Removal of ciprofloxacin from aqueous solution by a continuous flow electro-coagulation process

Jalal Basiri Parsa, Taher Mehdi Panah, and Farideh Nabizadeh Chianeh†

Department of Applied Chemistry, Faculty of Chemistry, University of Bu-Ali Sina, Hamadan, Iran
(*Received 21 February 2015 • accepted 9 September 2015*)

Abstract−This study deals with the performance and modeling of the electro-coagulation process for ciprofloxacin (CIP) removal by using aluminum electrode as anode in a continuous electrochemical reactor. The initial pH, temperature, current density, time and flow rate were selected as independent variables in response surface methodology (RSM) involving a five-level central composite design (CCD), while CIP removal efficiency was considered as the response function. The result of optimization showed that the maximum amount of CIP removal efficiency (88%) presented at the optimal condition of pH=5.6, t=100 min, T=25.5 °C, I=5.6 mA/cm^2 and V=25.9 mL/min. In addition, the mineralization of the CIP was investigated by chemical oxygen demand (COD) and total organic carbon (TOC) measurements that showed 77% COD removal and 49%TOC removal.

Keywords: Electro-coagulation, Ciprofloxacin, Response Surface Methodology, Continuous Flow Process

INTRODUCTION

Ciprofloxacin (CIP) is a broad-spectrum fluoroquinolone antimicrobial that can be used for complicated urinary tract and skin infections [1,2]. CIP has been found in wastewater treatment plants typically at concentrations of 11 to 99 μg L^{-1}, and up to 0.032 μg L^{-1} in raw drinking water [3-5]. CIP has low biodegradability and toxic effects on environmental bacteria. Therefore, this pollutant must be treated from drinking water and pharmaceutical factory effluent [1].

Many techniques including a pillared iron catalyst [6] ozone and photo processes [1], photo catalytic by ZnO nano-particles [7], photochemical method [8], photochemical by UV and UV/H_2O_2 [9], photolytic degradation [10], ozonation [11], photo Fenton process [12] have been developed to remove CIP from wastewater. However, most current technologies need chemical additives, harsh treatment conditions, high-energy consumption, and low mineralization degree.

Compared to other technologies, electro-coagulation (EC) process appears to be one of the most promising for removing recalcitrant organic pollutants from water because of its simplicity, ambient operability, reliability, cost-effectiveness, large volume handling ability, non-consumption of chemicals. In the EC process, the metal ions are actually generated through oxidation reaction, then the metal ions react with OH^- species that generated from hydrolysis reaction on cathode thereby producing $M(OH)_n$ [13]. In other words, the pollutants in electrochemical reactor are coagulated and removed by sedimentation and flotation. The proposed mechanism for the generation of coagulant agent is presented by the following equations[14]:

$$\text{Anode: } Al(s) \rightarrow Al^{3+}(aq) + 3e^- \quad (1)$$

$$\text{Cathode: } 3H_2O + 3e^- \rightarrow 3/2H_2\,(g) + 3OH^- \quad (2)$$

$$\text{In bulk: } Al^{3+}(aq) + 3H_2O \rightarrow 3/2\,H_2\,(g) + Al\,(OH)_3\,(s) \quad (3)$$

Our aim was to develop a simple, precise, reliable, and rapid stability flow method for the removal of CIP from aqueous solution. Although batch method has been successfully used for pollutants treatment, a continuous treatment method is worth to be tested. In this paper, an attempt is made to simulate the industrial design to a laboratory scale. The effect of concurrent five parameters on CIP removal process by response surface methodology (RSM) involving a five-level central composite design (CCD) was investigated. In many ways for experimental modeling, RSM is an effective tool for optimizing the process when a combination of several independent parameters and their interactions affect the desired responses.

EXPERIMENTAL

1. Materials and Instruments

The CIP, $C_{17}H_{18}FN_3O_3$, (CAS No.85721-33-1 and M_w=331.346 g/mol), was investigated as a model pollutant. The structure and

Table 1. CIP chemical structure and characteristics

Structure	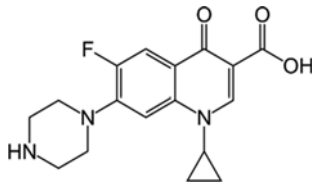
CAS number	85721-33-1
λ_{max} (nm)	274
M_w (g/mol)	331.346
pH	5.6

†To whom correspondence should be addressed.
E-mail: Nabizadeh_farideh@yahoo.com

Table 2. The central composite design matrix for five independent variables and experiments condition and response

Run	pH	T (C)	Time (min)	I (mA/cm^2)	V (mL/min)	R% (exp)	R% (pre)
1	8.70	29.00	77.00	6.20	57.00	83.00	81.72
2	5.30	29.00	77.00	6.20	102.00	86.00	84.55
3	8.70	51.00	77.00	3.70	57.00	46.00	46.62
4	5.30	51.00	102.00	3.70	57.00	57.00	58.01
5	8.70	29.00	77.00	3.70	102.00	63.00	62.55
6	5.30	29.00	102.00	3.70	102.00	80.00	79.43
7	7.00	40.00	89.50	4.95	79.50	71.00	72.56
8	5.30	51.00	102.00	3.70	102.00	55.00	55.62
9	5.30	51.00	77.00	3.70	102.00	43.00	44.96
10	5.30	29.00	102.00	6.20	57.00	86.00	87.10
11	5.30	29.00	102.00	3.70	57.00	83.00	82.82
12	7.00	40.00	119.23	4.95	79.50	76.00	75.99
13	8.70	29.00	102.00	6.20	102.00	79.00	77.75
14	7.00	40.00	89.50	4.95	79.50	71.00	72.56
15	7.00	40.00	89.50	4.95	79.50	72.00	72.56
16	5.30	29.00	77.00	3.70	102.00	67.00	68.01
17	8.70	51.00	102.00	3.70	102.00	50.00	49.65
18	7.00	40.00	89.50	4.95	79.50	74.00	72.56
19	7.00	40.00	89.50	4.95	79.50	72.00	72.56
20	5.30	51.00	77.00	3.70	57.00	45.00	45.34
21	8.70	29.00	77.00	6.20	102.00	79.00	79.83
22	7.00	66.16	89.50	4.95	79.50	35.00	33.21
23	7.00	40.00	89.50	4.95	79.50	75.00	72.56
24	7.00	13.83	89.50	4.95	79.50	83.00	84.18
25	7.00	40.00	89.50	7.92	79.50	75.00	75.42
26	7.00	40.00	59.77	4.95	79.50	64.00	63.41
27	8.70	29.00	77.00	3.70	57.00	67.00	67.18
28	8.70	29.00	102.00	6.20	57.00	83.00	81.63
29	7.00	40.00	89.50	4.95	79.50	72.00	72.56
30	5.30	29.00	77.00	3.70	57.00	70.00	69.40
31	8.70	29.00	102.00	3.70	102.00	70.00	69.96
32	5.30	51.00	77.00	6.20	57.00	59.00	60.63
33	7.00	40.00	89.50	4.95	133.01	70.00	70.16
34	8.70	51.00	102.00	3.70	57.00	55.00	55.29
35	7.00	40.00	89.50	4.95	79.50	74.00	72.56
36	11.04	40.00	89.50	4.95	79.50	61.00	62.27
37	8.70	51.00	102.00	6.20	57.00	61.00	61.82
38	7.00	40.00	89.50	4.95	25.98	76.00	75.24
39	5.30	29.00	77.00	6.20	57.00	82.00	83.19
40	8.70	51.00	102.00	6.20	102.00	59.00	58.94
41	2.95	40.00	89.50	4.95	79.50	73.00	71.12
42	5.30	51.00	77.00	6.20	102.00	64.00	62.99
43	5.30	29.00	102.00	6.20	102.00	86.00	86.47
44	8.70	51.00	77.00	3.70	102.00	44.00	42.99
45	7.00	40.00	89.50	4.95	79.50	73.00	72.56
46	8.70	51.00	77.00	6.20	57.00	63.00	62.66
47	5.30	51.00	102.00	6.20	57.00	65.00	63.79
48	8.70	29.00	102.00	3.70	57.00	76.00	76.60
49	8.70	51.00	77.00	6.20	102.00	61.00	61.77
50	7.00	40.00	89.50	4.95	79.50	72.00	72.56
51	5.30	51.00	102.00	6.20	102.00	63.00	64.16
52	7.00	40.00	89.50	1.97	79.50	49.00	47.98

characteristics of CIP are given in Table 1. De-ionized water was used for preparing the pollutant solutions. The pH of solutions was adjusted by using hydrochloric acid and sodium hydroxide, and sodium chloride was used as the supporting electrolyte. In all experiments, 2 g/L of sodium chloride was used for increasing conductivity of solutions.

The solution pH was measured by pH meter (Denver, UB-10). Master flex pump (ISMATEC-404B model) was applied to determine the flow rate. The CIP degradation was followed by using UV/Vis spectrophotometer (JASCO. v- 630, Japan). The chemical oxygen demand (COD) and total organic carbon (TOC) measurements were also carried out to investigate the mineralization of the solution, using a HACH DR 2800 as spectrophotometer and HACH DRB 200 as heater) and TOC analyzer (Multi n/c) purchased from Germany, respectively.

2. Experimental Design

We selected central composite design (CCD) to optimize the process and to determine the relationship between five operating variables, including initial pH (X_1), temperature (T (C^o)) (X_2), Time (t (min)) (X_3), current density (I (mA/cm^2)) (X_4), flow rate (V (mL/min)) (X_5). In the experimental design model, the initial pH, temperature, current density, time and flow rate were selected as independent variables, while CIP removal efficiency was considered as the response function. A total of 52 experiments were carried out, including 2^5=32 cube points, 2×5=10 axial points and 10 replications at the center point [15].

The Minitab software (16^{th} version) was used for regression and graphical analysis of the data obtained. For statistical calculations, the levels for the five main variables were coded as x_i according to the following equation [16]:

$$x_i = \frac{X_i - X_0}{\delta X} \quad (4)$$

where x_i is coded value of parameter X_i, X_0 is value of the parameter X_i at the center point and δX represents the step change value [17,18]. As usual, the experiments were performed in random order to avoid systematic error. Table 2 presents the central composite design matrix and comparison between the actual and the predicted response.

3. Experimental Procedure

All experiments were conducted in a reactor consisting of a double-wall cylinder with an internal volume of 500 mL. The outer layer was designed to regulate and maintain a constant temperature; this layer had an inlet pipe at the bottom and an outlet pipe on top the layer. Output water from the thermostat is linked into the inlet layer. Outlet water by silicon pipes returns to the thermostat again. The inside of the reactor consists of two-cathode electrodes 304 stainless steel with dimensions of 6 cm×2.7 cm and an aluminum anode with dimensions 6 cm×2.7 cm. In the reactor, the electrodes are aligned parallel to each other and separated a distance of 2 cm. The electric current is provided by a DC power supply (ADAK-PS-450). The flow rate of the influent was adjusted by a pump (Master flex ISMATEC-404B). The schematic of the electrochemical cell is shown in Fig. 1. In each experiment, current density, initial pH, temperature, time and flow rate values were adjusted according to Table 2. After a certain time proposed in Table 2, 5 mL of sample was collected, centrifuged for 5 min, and analyzed by UV-Vis spectrophotometer (JASCO. v- 630, Japan).

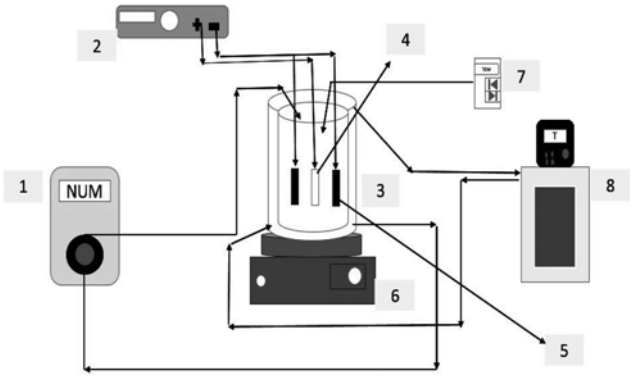

Fig. 1. Schematic of electrochemical cell.

1. Circulator pump
2. DC power supply
3. Reactor
4. Anode Al
5. Cathode ss-304
6. Stirrer
7. Thermometer
8. Thermostat

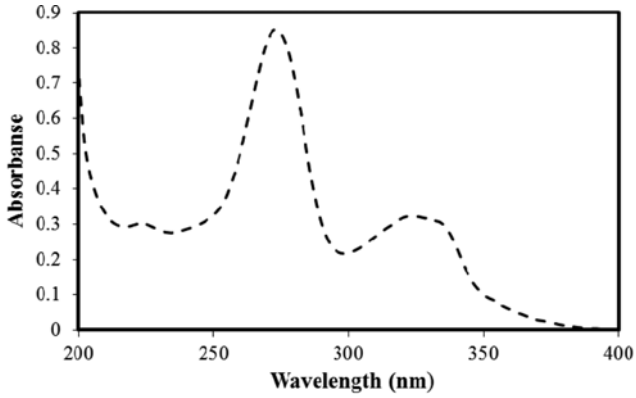

Fig. 2. Ciprofloxacin UV/Vis spectra ([CIP]=10 mg/L, T=25 °C).

4. UV/Vis Spectra

CIP absorption spectrum has a maximum absorption wavelength at 274 nm and it has a weak peak in 321 that relates to electron transport [19]. The CIP UV/V spectrum is shown in Fig. 2. The CIP removal efficiency was determined using the following equation.

$$X = \frac{A_0 - A_t}{A_0} \quad (5)$$

In this equation, A_0 and A are initial and final CIP absorbance in the synthetic wastewater.

RESULTS AND DISCUSSION

1. Optimization of EC Treatment of CIP

The general structure of the second-order mathematical model, used in the response surface analysis, can be explained by the following quadratic equation [15]:

$$Y = b_0 + \Sigma b_i x_i + \Sigma b_{ii} x_i^2 + \Sigma b_{ij} x_i x_j \quad (6)$$

where Y is the value of the CIP removal efficiency, b_0 is a constant,

b_i is the linear coefficient, b_{ii} is the quadratic coefficients, b_{ij} is the interaction coefficients, and x_i (x_j) is the coded experimental levels of the design variables.

The experimental design matrix together with the observed and predicted CIP removal efficiencies is given in Table 2. Based on these results, the second-order polynomial equation for CIP removal efficiency in terms of coded factors was obtained in the form of following equation (Eq. (7)):

$$\begin{aligned} Y_{pre} = {} & 72.5601 - 1.8595x_1 - 10.7163x_2 + 2.6445x_3 + 5.7681x_4 - 1.0683x_5 \\ & - 1.0366x_1^2 - 2.4508x_2^2 - 0.5063x_3^2 - 1.9205x_4^2 + 0.0241x_5^2 \\ & + 0.8750x_1x_2 - 1.0000x_1x_3 + 0.1875x_1x_4 - 0.8125x_1x_5 \\ & - 0.1875x_2x_3 + 0.3750x_2x_4 + 0.2500x_2x_5 - 2.3750x_3x_4 \\ & - 0.5000x_3x_5 + 0.6875x_4x_5 \end{aligned} \quad (7)$$

The significance and adequacy of the model was evaluated through ANOVA (analysis of variance) [20,21]. As can be seen from Table 3, the quadratic model has an R^2 value of 0.9928, which is very high and expresses a high correlation between the obtained and predicted values. Additionally, the predicted R^2 (0.9777) was in acceptable agreement with the adjusted R^2 of 0.9882. Therefore, the response surface model was accurately applied for predicting the behavior of the process [22].

Table 3. ANOVA table for fit of CIP removal efficiency from central composite design

Source of variations	Degree of freedom	Seq SS	Adj SS	Adj MS	F-value
Regression	20	7771.51	7771.51	388.58	214.11
Residuals	31	56.26	56.26	1.81	
Total	51	7827.77			
R-sq=0.9928		R-sq(pre)=0.9777		R-sq(adj)=0.9882	

Table 4. Estimated regression coefficients and corresponding F and P values from the data of central composite design experiments

Coefficient	Parameters estimate	F-value	P-value
b_0	72.5601	762.31	0.000
b_1	−1.8595	82.52	0.000
b_2	−10.7163	2740.84	0.000
b_3	2.6445	166.90	0.000
b_4	5.7681	794.07	0.000
b_5	−1.0683	27.24	0.000
b_1^2	−1.0366	34.65	0.000
b_2^2	−2.4508	193.71	0.000
b_3^2	−0.5063	8.27	0.007
b_4^2	−1.9205	118.94	0.000
b_5^2	0.0241	0.02	0.892
b_1b_2	0.8750	13.50	0.001
b_1b_3	−1.0000	17.63	0.000
b_1b_4	0.1875	0.62	0.437
b_1b_5	−0.8125	11.64	0.002
b_2b_3	−0.1875	0.62	0.437
b_2b_4	0.3750	2.48	0.125
b_2b_5	0.2500	1.10	0.302
b_3b_4	−2.3750	99.46	0.000
b_3b_5	−0.5000	4.41	0.044
b_4b_5	0.6875	8.33	0.007

Estimated regression coefficients and corresponding F and P-values for CIP are shown in Table 4. The P-values were used to check the significance of each variables interaction and parameters interaction importance. The F-values can be used for adaptability between actual value and predicted value for each parameter and their interaction [23]. A P-value more than 0.05 shows the parameter interaction does not have a significant effect on treatment removal [24]. Also, value of lack of fit (>0.05) is non-significant, which indicates that the quadratic model is statistically significant for the response [15]. According to the correlation coefficient value, the regression line is perfectly fitted with the experimental points.

The residuals plot is an important diagram for evaluating the proportionality and adequacy of the developed model. The residuals plot for CIP removal efficiency is shown in Fig. 3(a). Based on this plot, the residuals (difference between the observed and the predicted response values) change in a random pattern around the centerline and the response follows the fitted normal distribution.

Fig. 3(b) shows the actual values compared to the predicted values calculated by using the resulting second-order polynomial equation (Eq. (7)). This plot has correlation coefficient of 0.992. All points are reasonably close to a straight line and confirm that the actual values are in good agreement with the predicted values [16,25,26] .

Pareto plot shows the impact of parameters and their interaction as a percentage, on the response. This parameter can be calculated as the following equation [27]:

$$P = \left(\frac{b_i^2}{\sum b_i^2} \right) \times 100 \quad (8)$$

As can be seen from Fig. 4, the effect variables and interactions are ordered according to their relative importance, and temperature (b_5=63.8%) and current density (b_2=18.50%) are the most significant factors on CIP removal efficiency. However, temperature has negative effect, but current intensity has positive effect.

2. Effect of Operational Parameters

Fig. 5 illustrates the effect of pH and T on CIP removal efficiency for time, current density, and flow rate of 89.5 min, 4.95 mA/cm^2, and 79.5 mL/min, respectively. This figure shows that the CIP removal efficiency decreased with the increase in pH and temperature. As shown, CIP removal efficiency decreased with increasing pH at all temperatures. However, at high temperatures, effect of increasing pH on CIP removal efficiency was less significant. This result can be interpreted based on this reason that, in high pH, $Al(OH)_3$ has a soluble form ($Al(OH)_4^-$) which cannot be adsorbed the CIP species [28]. In acidic pH, aluminum complexes have Al^{3+}, AlO^+ and $AlOH^{2+}$ forms and these forms cannot pollutant be absorbing. In addition, for pH between 5 and 8, aluminum complex dissolution decreases and the pollutant adsorption increases [29]. Ouaissa et al. also found similar results for the removal of tetracycline (TC) [34]. As can be seen from Fig. 5, increasing the temperature reduces CIP removal efficiency. In electrochemical processes, pollutant removal efficiency depends on the temperature of the solution and the increasing temperature results in the pollut-

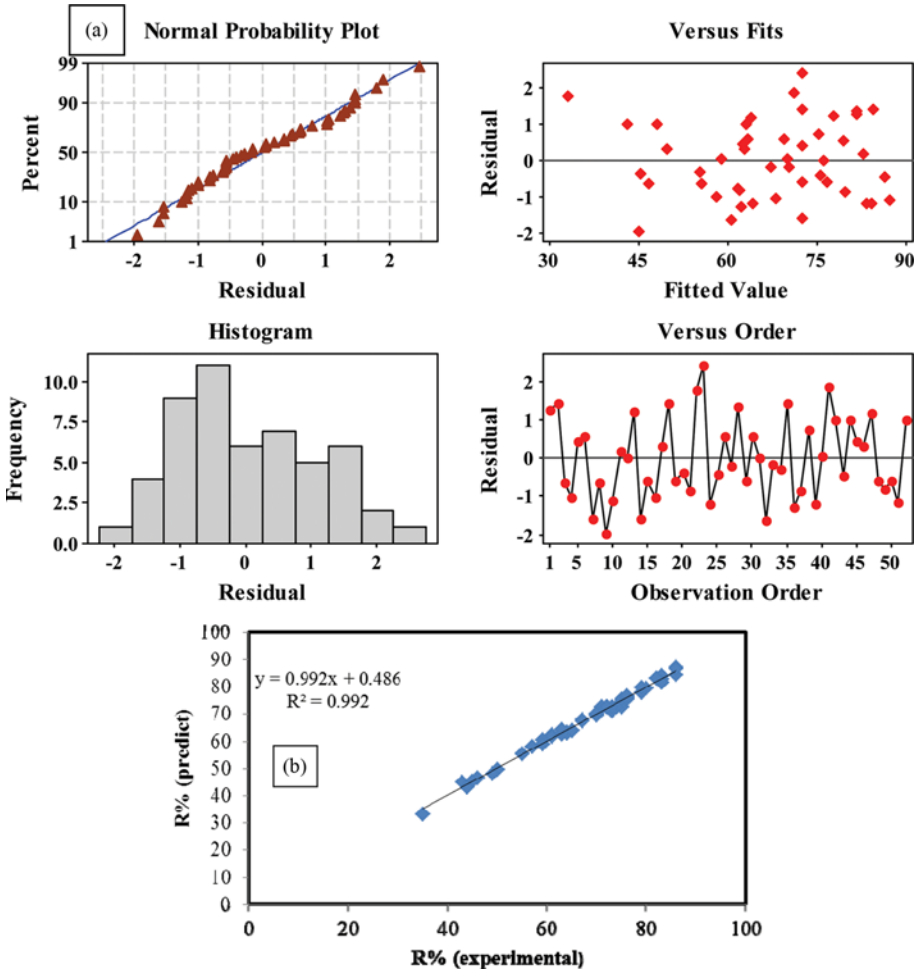

Fig. 3. (a) Residual plots for CIP removal efficiency, (b) the experimental values (%) plotted against the predicted values (%) derived from the central composite design resulted equation.

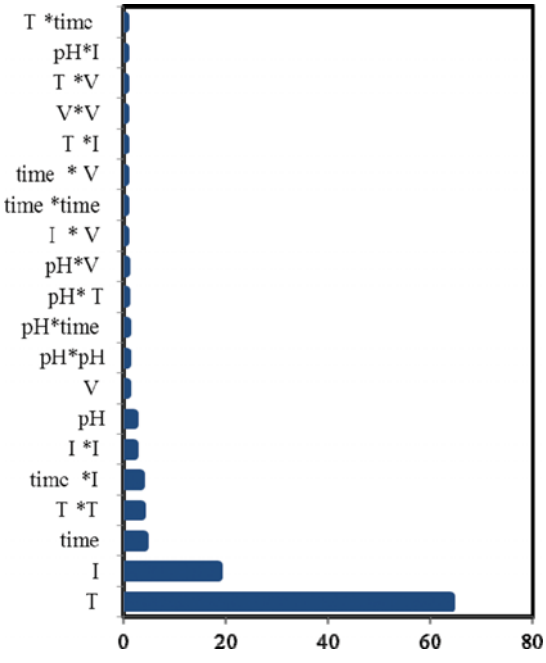

Fig. 4. Pareto graphic analysis.

ant removal efficiency increases. However, at high temperatures, an increase in the solubility of the precipitates, leads to the decreasing of the pollutant removal efficiency [30]. In other words, at high temperatures, the sediment was dissolved and increased the speed of flotation and reduced the adhesion of coagulant, which could have occurred because production of larger hydrogen bubbles was increased. At low temperature, CIP treatment curve trend is descending because at low temperature coagulant agent was not formed and mass transfer in solution is low [16,31].

Fig. 6 shows the response surface and contour plots of the CIP removal efficiency as a function of time and pH. As shown in this figure, suitable range for pH is (5-8). The reason for this observation was explained in the previous paragraphs. Because of great interest in applying mild condition of natural pH (pH_{CIP}=5.6), there was no need to add acids or bases into the solution; a pH of 5.6 was preferred as optimum pH. In electro-coagulation process, the pollutant removal efficiency depends directly on the ion concentration of the solution. In this plot as will be seen, with increasing the time, the degradation is increased because coagulant concentration is increasing in solution [32]. Varank et al. also found similar results for treatment of tannery wastewater [33].

Fig. 7 shows the effect of pH and Von CIP removal efficiency.

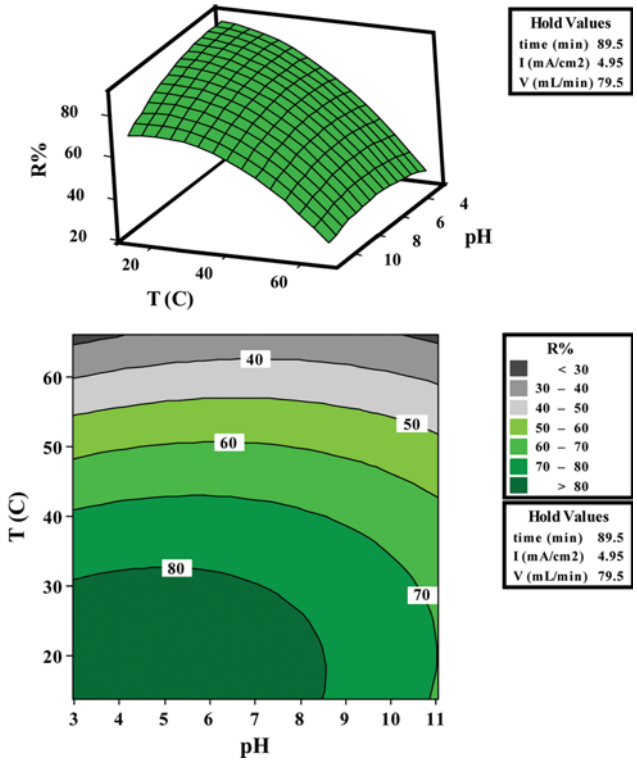

Fig. 5. The response surface plot and contour plot of the CIP removal as function of temperature and pH.

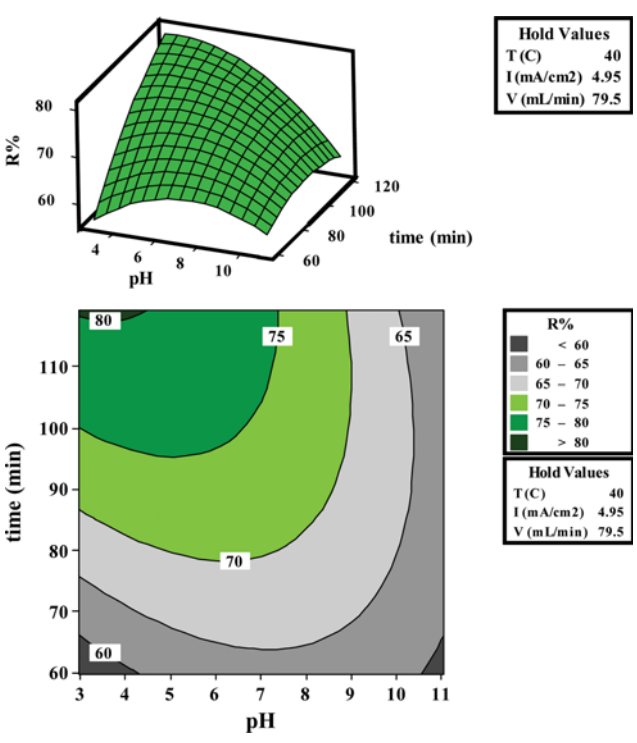

Fig. 6. The response surface plot and contour plot of the CIP removal as function of time and pH.

CIP removal has descending trend with increasing the pH. CIP removal efficiency increases with decreasing the flow rate because

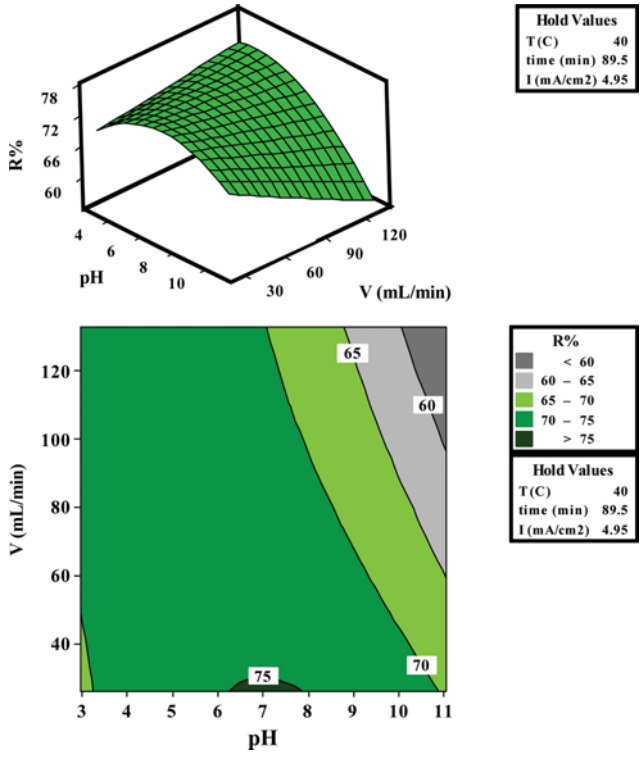

Fig. 7. The response surface plot and contour plot of the CIP removal as function of flow rate and pH.

at high flow rate the EC process has a turbulent environment and this condition leads to unsuitable interaction between coagulant and pollutant [34]. Actually, the flow rate refers to the residence time in the reactor, so increasing of residence time is equal to decreasing of flow rate, and this action causes an increasing of the amount of electro-generated Al^{3+}. The flow rate determines the contact time between flocs and pollutants. Lu et al. also found similar results for removal of heavy metal ions with continuous aluminum electro coagulation; their results showed that the degree of pollutant treatment was dependent on both fluid dynamics and mass transfer, which it decreases with the increment of flow rate [35,36].

The performance of the EC process depends on the amount of coagulant produced or applied charge loading [37]. In flow process, investigation of current density and residence time influence was necessary. Current density has a great impact on pollutant removal after temperature. In Fig. 8, the interaction between V and I and their effect on CIP removal efficiency is shown. As can be seen, CIP degradation increases with increasing the current density. The enhancement in CIP removal efficiency with the increase current density can be associated with a greater production of Al^{3+}, which leads to a greater amount of precipitate for adsorption of CIP species [38,39].

This figure represents that the CIP removal efficiency does not depend to a large extent on flow rate. Therefore, the suitable range is the slowest flow rate and CIP removal efficiency slightly increases with the increase of flow rate.

Fig. 9 shows the response surface and contour plots for CIP removal efficiency as a function of flow rate and time at pH, current density, and temperature of 7, 4.95 mA/cm^2 and 40 C^0, respectively.

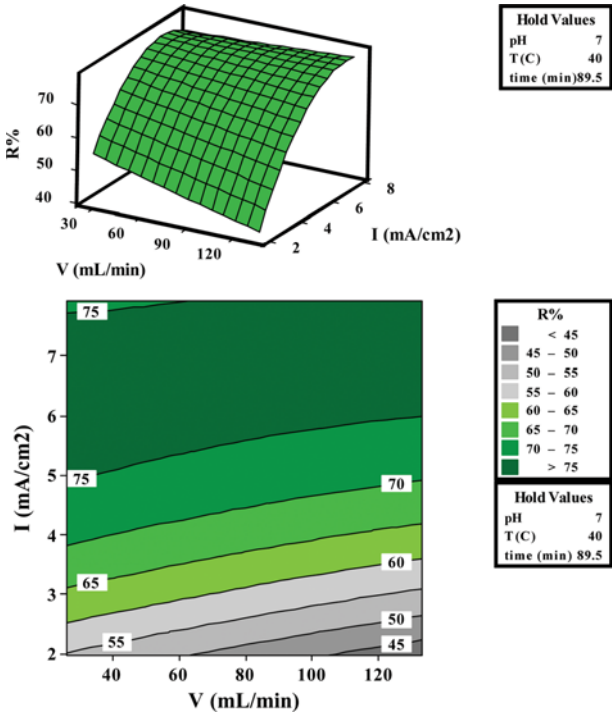

Fig. 8. The response surface plot and contour plot of the CIP removal as function of current density and pH.

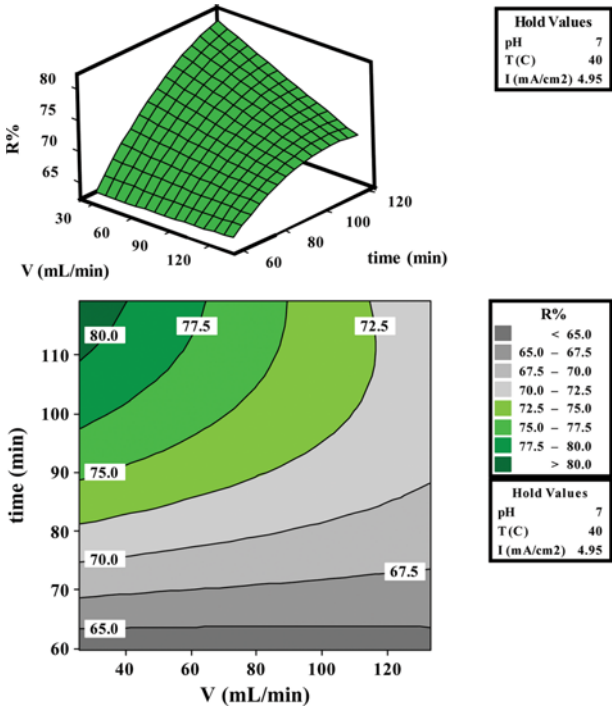

Fig. 9. The response surface plot and contour plot of the CIP removal as function of flow rate and time.

As can be seen from Fig. 9, CIP removal efficiency increases with the increase of the reaction time because of greater production of coagulant species [40].

3. Determination of Optimal Conditions for Removal of CIP

The main objective of the optimization is to determine the optimum values of variables and to achieve maximum treatment performance. The optimum values are shown in Table 5. Under these optimum conditions, a specific experiment was carried out; the results showed the CIP removal efficiency obtained from the experiment and as estimated by quadratic model was satisfactory.

4. Investigation of UV/Vis Spectra, COD, and TOC Removal in Optimizing Experiment

Under optimized conditions, UV/Vis spectra, COD, and TOC removal were investigated. Results are shown in Figs. 10, 11 and 12. Comparison between UV/Vis spectra (88% CIP removal efficiency), COD removal (77%), and TOC removal (49%) indicates that the process was successful in removing the carbonyl functional

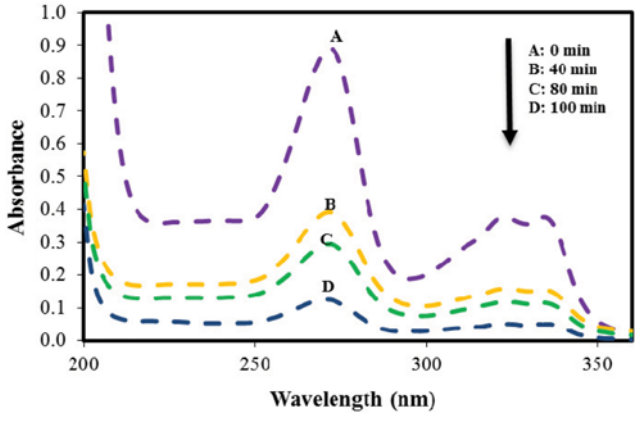

Fig. 10. CIP removal trend following by UV/Vis spectrum at {[CIP]= 10 mg/L, pH=5.6, T=25.5 °C, I=5.6 mA/cm^2 and V=25.9 mL/min}.

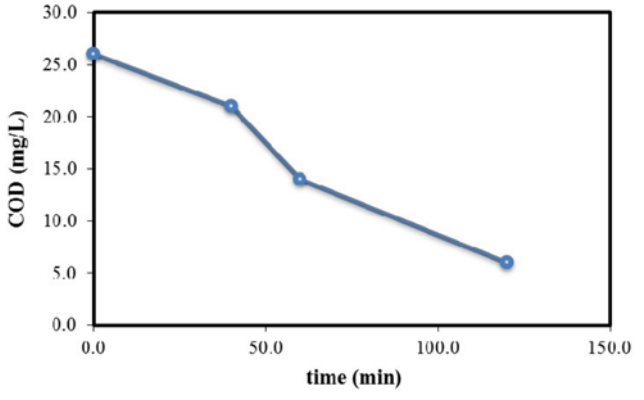

Fig. 11. COD removal trend for CIP treatment at {[CIP]=10 mg/L, pH=5.6, T=25.5 °C, I=5.6 mA/cm^2 and V=25.9 mL/min}.

Table 5. Optimal condition and comparison between actual value and predicted value

Parameters	pH	T (°C)	Time (min)	I (mA/cm^2)	V (mL/min)	R% (pre)	R% (exp)
Optimal value	5.6	25.5	100	5.6	25.9	90.14	88

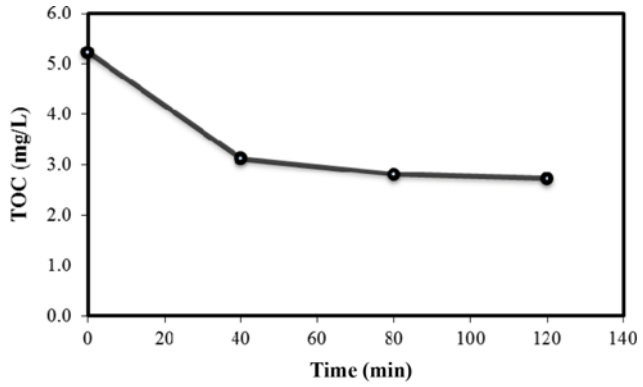

Fig. 12. TOC removal trend for CIP treatment at {[CIP]=10 mg/L, pH=5.6, T=25.5 °C, I=5.6 mA/cm^2 and V=25.9 mL/min}.

group; however, less organic carbon was removed.

CONCLUSION

The removal of the CIP in aqueous solution was investigated by using aluminum electrode as anode in a continuous electrochemical reactor. Central composite design (CCD) was applied to model process and to evaluate the effect of independent variables (initial pH, temperature, current density, time and flow rate) on the CIP removal efficiency. The optimum values of the pH, current density, flow rate, temperature and reaction time were 5.6, 5.6 mA/cm^2, 25.9 mL·min^{-1}, 25.5 °C and 100 min, respectively. At optimized conditions, 88% CIP removal efficiency, 77% COD removal and 49% TOC removal efficiency were obtained. Based on analysis of variance (ANOVA), the coefficient of determination value (R^2=0.9928) was high, showing a satisfactory adjustment of the actual data with the predicted data

ACKNOWLEDGEMENTS

The authors thank the University of Bu-Ali Sina, Iran for financial and other support.

NOMENCLATURE

EC : electro-coagulation
CIP : ciprofloxacin
RSM : response surface methodology
CCD : central composite design
COD : chemical oxygen demand
TOC : total organic carbon
A_0 : initial CIP absorbance
A : final absorbance of CIP solution
V : flow rate [mL/min]
T : temperature [C^0]
I : current density [mA/cm^2]

REFERENCES

1. T. G. Vasconcelos, K. Kummerer, D. M. Henriques and A. F. Martins, *J. Hazard. Mater.*, **169**, 1154 (2009).
2. X. Van Doorslaer, K. Demeestere, P. M. Heynderickx, H. Van Langenhove and J. Dewulf, *Appl. Catal. B: Environ.*, **101**, 540 (2011).
3. T. G. Vasconcelos, D. M. Henriques, A. Konig, A. F. Martins and K. Kummerer, *Chemosphere*, **76**, 487 (2009).
4. M. Seifrtova, A. Pena, C. M. Lino and P. Solich, *Anal. Bioanal. Chem.*, **391**, 799 (2008).
5. B. Morasch, F. Bonvin, H. Reiser, D. Grandjean, L. F. de Alencastro, C. Perazzolo, N. Chevre and T. Kohn, *Environ. Toxicol. Chem.*, **29**, 1658 (2010).
6. M. Bobu, A. Yediler, I. Siminiceanu and S. Schulte-Hostede, *Appl. Catal B: Environ.*, **83**, 15 (2008).
7. M. El-Kemary, H. El-Shamy and I. El-Mehasseb, *J. Lumin*, **130**, 2327 (2010).
8. F. Hernández, A. Rivera, A. Ojeda, T. Zayas and L. Cedillo, *J. Environ. Sci. Eng. A*, **1**, 448 (2012).
9. H. G. Guo, N. Y. Gao, W. H. Chu, L. Li, Y. J. Zhang, J. S. Gu and Y. L. Gu, *Environ. Sci. Pollut. Res. Int.*, **20**, 3202 (2013).
10. S. Babic, M. Perisa and I. Skoric, *Chemosphere*, **91**, 1635 (2013).
11. C. Liu, V. Nanaboina, G. V. Korshin and W. Jiang, *Water Res.*, **46**, 5235 (2012).
12. J. A. de Lima Perini, M. Perez-Moya and R. F. P. Nogueira, *J. Photochem. Photobiol. A*, **259**, 53 (2013).
13. P. Cañizares, M. Carmona, J. Lobato, F. Martínez and M. A. Rodrigo, *Ind. Eng. Chem. Res.*, **44**, 4178 (2005).
14. J. B. Parsa and F. N. Chianeh, *Korean J. Chem. Eng.*, **29**, 1585 (2012).
15. F. Nabizadeh Chianeh and J. Basiri Parsa, *Chem. Eng. Res. Des.*, **92**, 2740 (2014).
16. A. R. Khataee, M. Zarei and L. Moradkhannejhad, *Desalination*, **258**, 112 (2010).
17. R. Lopez-Serna, M. Petrovic and D. Barcelo, *Chemosphere*, **85**, 1390 (2011).
18. J. P. Kushwaha, V. C. Srivastava and I. D. Mall, *Sep. Purif. Technol.*, **76**, 198 (2010).
19. D. L. Pavia, G. M. Lampman and G. S. Kriz, Harcourt. Brace. College. Publishers (1996).
20. S. Ghafari, H. A. Aziz, M. H. Isa, A.A. *J. Hazard. Mater.*, **163**, 650 (2009).
21. M. B. Kasiri and A. R. Khataee, *Desalination*, **270**, 151 (2011).
22. P. Sharma, L. Singh and N. Dilbaghi, *J. Hazard. Mater.*, **161**, 1081 (2009).
23. K.-W. Pi, Q. Xiao, H.-Q. Zhang, M. Xia and A. R. Gerson, *Process. Saf. Environ*. (2014), DOI:10.1016/j.psep.2014.02.008.
24. I.-H. Cho and K.-D. Zoh, *Dyes Pigm.*, **75**, 533 (2007).
25. S. Madaeni, N. Arast, F. Rahimpour and Y. Arast, *Desalination*, **280**, 305 (2011).
26. Y. Wu, S. Zhou, F. Qin, X. Ye and K. Zheng, *J. Hazard. Mater.*, **180**, 456 (2010).
27. L. Wei, H. Zhu, X. Mao and F. Gan, *Sep. Purif. Technol.*, **77**, 18 (2011).
28. J. B. Parsa, H. R. Vahidian, A. Soleymani and M. Abbasi, *Desalination*, **278**, 295 (2011).
29. C. Jiménez, C. Sáez, F. Martínez, P. Cañizares and M. A. Rodrigo, *Sep. Purif. Technol.*, **98**, 102 (2012).
30. S. Song, Z. He, J. Qiu, L. Xu and J. Chen, *Sep. Purif. Technol.*, **55**, 238 (2007).

31. B. Khaled, B. Wided, H. Béchir, E. Elimame, L. Mouna and T. Zied, *Arabian J. Chem.*, DOI:10.1016/j.arabjc.2014.12.012.
32. S. Zhang, J. Zhang, W. Wang, F. Li and X. Cheng, *Sol. Energy Mater. Sol. C*, **117**, 73 (2013).
33. G. Varank, H. Erkan, S. Yazýcý, A. Demir and G. Engin, *Int. J. Environ. Res.*, **8**, 165 (2014).
34. S. Zodi, B. Merzouk, O. Potier, F. Lapicque and J.-P. Leclerc, *Sep. Purif. Technol.*, **108**, 215 (2013).
35. N. S. Kumar and S. Goel, *J. Hazard. Mater.*, **173**, 528 (2010).
36. J. Lu, Y. Li, M. Yin, X. Ma and S. Lin, *Chem. Eng. J.*, **267**, 86 (2015).
37. M. Kobya, F. Ulu, U. Gebologlu, E. Demirbas and M. S. Oncel, *Sep. Purif. Technol.*, **77**, 283 (2011).
38. Y. A. Ouaissa, M. Chabani, A. Amrane and A. Bensmaili, *J. Environ. Chem. Eng.*, **2**, 177 (2014).
39. A. Attour, M. Touati, M. Tlili, M. Ben Amor, F. Lapicque and J.-P. Leclerc, *Sep. Purif. Technol.*, **123**, 124 (2014).
40. S. Bayar, A. E. Yilmaz, R. Boncukcuoğlu, B. A. Fil and M. M. Kocakerìm, *Desalin. Water Treat.*, **51**, 2635 (2013).